

# Preparation of concentrated aqueous alumina suspensions for soft-molding microfabrication

Dou Zhang, Bo Su, Tim W. Button\*

*IRC in Materials Processing, School of Engineering, the University of Birmingham, Edgbaston, Birmingham B15 2TT, UK*

## Abstract

This paper reports the preparation of highly concentrated aqueous alumina suspensions for demonstrating the microfabrication of ceramics by using soft molds of Poly(dimethyl siloxane) (PDMS) instead of the traditional solid molds. Zeta potential measurements showed very good dispersing effects of the dispersant  $\text{NH}_4\text{PAA}$ . The rheological properties of concentrated aqueous alumina suspensions have been characterized with varying pH,  $\text{NH}_4\text{PAA}$  concentration, solids loading and ultrasonic processing time. The intrinsic pH of the suspension was found suitable for molding. The optimum dispersant concentration is 0.14 wt.% and viscosities increase with more  $\text{NH}_4\text{PAA}$ . A stable and easily processable suspension of 84.0 wt.% was achieved and suitable for soft-molding with viscosity of 0.30 Pa s at  $100 \text{ s}^{-1}$ . Embossing and microtransfer molding have been used for soft-molding microfabrication and finally, crack-free and dense microstructures have been fabricated successfully with feature sizes of  $\sim 30 \mu\text{m}$ .

© 2003 Elsevier Ltd. All rights reserved.

**Keywords:**  $\text{Al}_2\text{O}_3$ ; Microfabrication;  $\text{NH}_4\text{PAA}$ ; PDMS; Soft-molding

## 1. Introduction

The development of microelectronic technologies is central to modern science and technology. The micro-fabrication of sensors and actuators<sup>1,2</sup> is one of the most promising applications, such as microanalysis,<sup>3</sup> micro-volume reactors<sup>4</sup> and microelectromechanical systems (MEMS).<sup>5,6</sup> However, most of them are made by silicon-based microfabrication techniques. In severe environments such as high temperature, high pressure or chemical corrosion, ceramics show very good thermal, mechanical or chemical inertness properties. Moreover, the unique magnetic, piezoelectric or electro-optical properties offer ceramics a lot of applications. Obviously it is very important to fabricate or integrate ceramics into micrometer-sized systems.<sup>7,8</sup>

Recent development of ceramic microfabrication techniques are either from the traditional IC techniques, such as wet etching<sup>9,10</sup> and dry etching,<sup>9,11,12</sup> which requires the compatibility between materials system and etchants, or trying to downsize the current ceramic forming techniques, such as co-extrusion,<sup>13</sup> slip casting,<sup>14</sup> injection molding<sup>15</sup> and rapid prototyping<sup>16,17</sup>

which includes three dimensional printing (3DP),<sup>18</sup> suspension printing<sup>19</sup> or ink-jet printing,<sup>20,21</sup> stereolithography<sup>22,23</sup> and selective laser sintering (SLS).<sup>24,25</sup> For example, a modified pressure assisted slip casting<sup>26</sup> consolidating the  $\text{Al}_2\text{O}_3$  slip in a compaction tool with a non-porous PMMA mold while the liquid being forced through the filter and the duct, was used for micro-fabrication of column and nozzles with some 10 microns size and high aspect ratio, but only suited for thin wall thickness structures and disk-like substrates. Some researchers used the photoresist structures patterned by standard ultraviolet lithography techniques as the molds for casting the ceramic suspensions or ceramic polymer precursor, combined with the lost-mold method to release the structures by either pyrolysis decomposition or chemical dissolution of the photoresist.<sup>7,27</sup>

In contrast, instead of the solid molds, soft molds that were replicated from a master like SU-8 photoresist (a negative, epoxy-type, near-UV photoresist) were used in this study. Poly(dimethylsiloxane) (PDMS) polymer is very suitable for the soft molds<sup>28,29</sup> due to its low interfacial free energy, chemical inertness and very good durability which allows it to be used many times.

Aqueous alumina suspensions have been well characterized by many researchers for slip casting, tape casting or spray drying. In order to obtain the highest green density and reduce the final shrinkage of the

\* Corresponding author. Tel.: +44-121-414-5237; fax: +44-121-414-7639.

E-mail address: [t.w.button@bham.ac.uk](mailto:t.w.button@bham.ac.uk) (T.W. Button).

micrometer sized components with good precision and homogeneity, the use of fine powders is required and the solids loading of the suspension must be as high as possible while the viscosity should be kept low enough for processing.

When ceramic powders are added to a solvent such as water, attractive Van der Waals forces can make the powders aggregate to form clusters, resulting in a relatively high suspension viscosity and difficulty in processing, and leading to flaws in the final sintered body. However, the agglomerate system can be dispersed to be relatively fluid and homogeneous by the introduction of repulsive forces between particles, including electrostatic repulsion of surface charges, steric repulsion, where absorbed polymer molecules physically prevent particles coming close enough for the Van der Waals attractive force to dominate, and electrosteric repulsion, which is a combination of the other two mechanisms.<sup>30–33</sup>

In this paper, alumina suspensions with high solids loadings, suitable viscosity and colloidally stable were studied for the soft molding of fine ceramic components in the range of micrometer sizes, which normally are very difficult and expensive to realize by traditional fabrication techniques such as photolithography and micromachining.

## 2. Experimental

### 2.1. Molds

The elastomeric molds were fabricated from PDMS. The master was placed in a glass petri dish. A 10:1 (weight ratio) mixture of PDMS-Sylgard Silicone Elastomer 184 and Sylgard Curing Agent 184 (Dow Corning Corp.) was mixed and left for half an hour while most of the gas bubbles vanished from the solution. Then the mixture was poured onto the master template in a vacuum desiccator. The templates were placed in such a vacuum condition for about half an hour to remove the residual gas bubbles. The PDMS was cured at 65 °C for 4 h according to the recommended schedule of Dow Corning. After cooling to room temperature, the rigid PDMS was carefully peeled from the master template.

### 2.2. Suspension preparation

The alumina suspensions were prepared by adding A-16 SG alumina powder [Alcoa Manufacturing (GB) Ltd, Worcester, UK] to the mixture of distilled water (17 M $\Omega$ ·cm) and the ammonium polyacrylate (NH<sub>4</sub>PAA) solution (Dispex A40, Allied Colloids, Bradford, UK, a 37.6% concentrated solution of average molecular weight 3500 g mol<sup>-1</sup>) under constant stirring. All samples were weighed to  $\pm 0.001$  g and typical batch size was 50 g. Any pH adjustments

required were made using 1 M HCl and concentrated (35%) NH<sub>4</sub>OH. The suspensions were ball milled with zirconia balls for 15 h. Two drops of 1-octanol were added to reduce the surface tension of the suspension. Finally, the suspensions were left for 24 h for the removal of air bubbles before rheological testing and microfabrication. The amount of NH<sub>4</sub>PAA used here is expressed as a dry weight of the powder basis (dwb), equivalent to the wt./wt. basis of the alumina powder.

Zeta potentials were measured for 180 ml, 3.33 wt.% suspensions with the variation of pH and added dispersant, Dispex A40, using Acoustosizer II (Colloidal Dynamics, USA). The pH was adjusted with 1 M HCl and concentrated NH<sub>4</sub>OH.

The rheological behaviour of the suspensions was studied using the CSL Rheometer (Carri-med 115/A) with the cone and plane system (Truncation: 55 microns; Core: 4 cm, 20°) at the temperature of 20 °C.

### 2.3. Soft molding and sintering

Schematic procedures of soft molding are shown in Fig. 1, and (a) is embossing and (b) is microtransfer molding ( $\mu$ TM), respectively. For embossing, alumina substrates were cleaned using acetone and ethanol followed by dropping the suspensions on the substrate, then the mold was quickly placed face down on the surface. A pressure was applied to carefully push the air bubbles out. For  $\mu$ TM, the suspensions were dropped on the patterned surface of a PDMS mold and the excess was removed by scraping with a flat PDMS

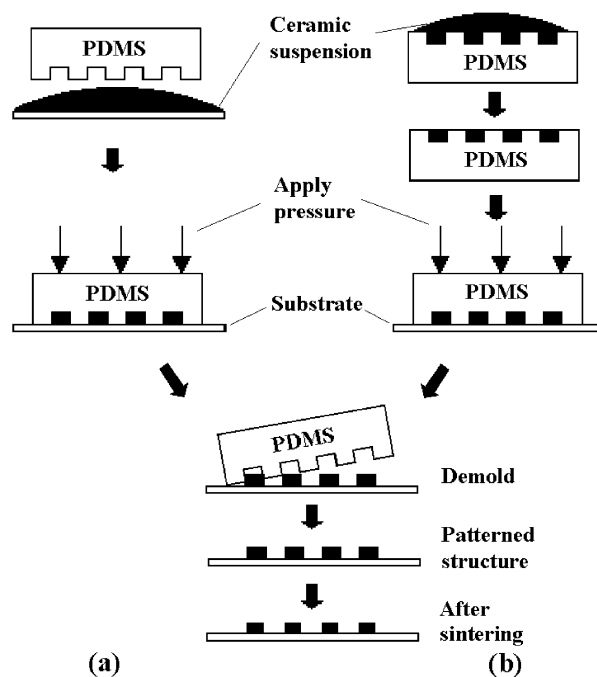


Fig. 1. Schematic procedures of soft molding: (A) embossing; (B) microtransfer molding ( $\mu$ TM).

block. The filled mold was then placed in contact with the freshly cleaned substrate and a little pressure was applied. After drying from the procedures as above, the PDMS molds were carefully peeled off from the alumina substrate. The PDMS molds were cleaned by an ultrasonic processor in distilled water and ethanol, respectively, and ready to reuse. Sintering was done at 1550 °C for 2 h.

### 3. Results and discussion

Fig. 2 shows the transmission electron microscopy (TEM) photo of the alumina powder used in this study, showing the particle size around 0.5  $\mu\text{m}$ . The specific surface area of the alumina powder is 9.09  $\text{m}^2/\text{g}$  measured by BET single point nitrogen adsorption experiment (Norcross, USA).

The IEP where the zeta potential was zero occurred at  $\text{pH} = 8.5$  for the 3.33 wt.% alumina suspension without dispersant A40, shown in Fig. 3. And at low pH, the curve showed the particles were highly positively charged. Fig. 4 shows the intrinsic pH of the suspension without dispersant A40 was 9.1 with zeta potential of  $-13.9$  mV, indicating a negatively charged surface con-

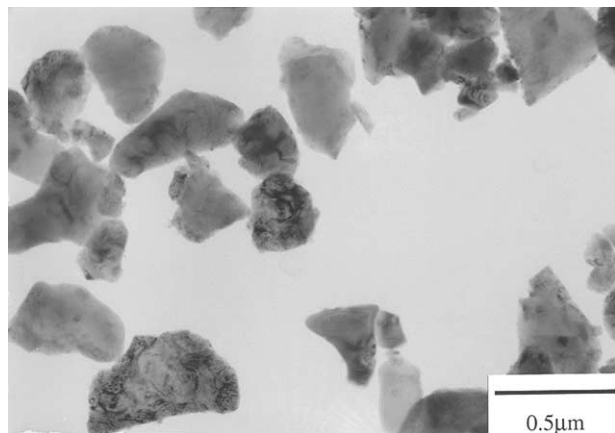


Fig. 2. TEM photo of the A-16 SG alumina powder.

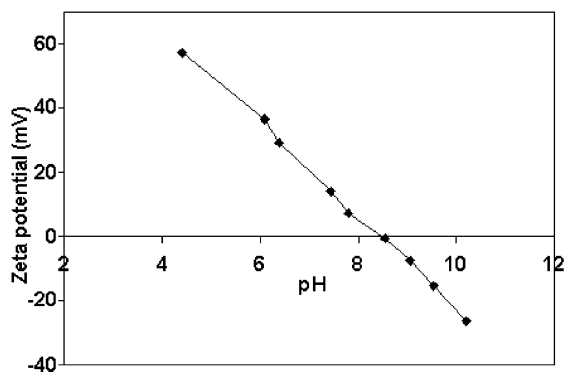


Fig. 3. Zeta potential vs. pH of 3.33 wt.% alumina suspension without dispersant.

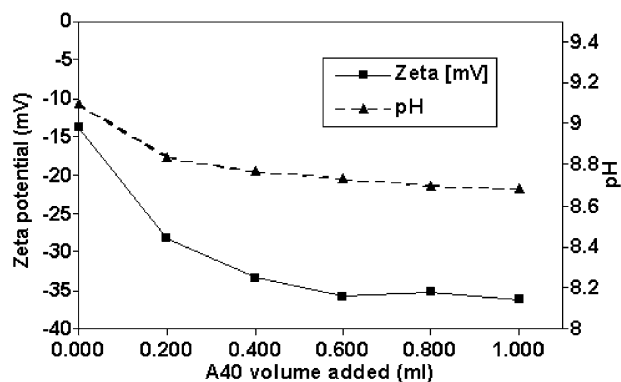


Fig. 4. Zeta potential and pH of 3.33 wt.% alumina suspension vs the amount of Dispers A40.

dition and an excess of  $\text{AlO}^-$  sites. The addition of dispersant  $\text{NH}_4\text{PAA}$  to the suspension caused the zeta potential to become more negative, from  $-13.9$  mV to around  $-35.9$  mV, showing the very good dispersing effect of A40 at this intrinsic pH. And the slight decrease of pH while adding dispersant A40 indicated a weak acid property of  $\text{NH}_4\text{PAA}$ .

Fig. 5 shows the change of the viscosity of a 75.0 wt.%, 0.14 wt.%  $\text{NH}_4\text{PAA}$  alumina suspension with decreasing the pH. The intrinsic pH of the suspension was 10.0, and the IEP was around 7.0. Compared with the IEP of the suspension without dispersant in Fig. 3, the shift towards lower pH values as increasing  $\text{NH}_4\text{PAA}$  reflects the adsorption of  $\text{NH}_4\text{PAA}$  on the alumina powders and hence increasing the negative surface charge. Being a polyelectrolyte,  $\text{NH}_4\text{PAA}$  was used to provide the electrosteric stabilization energy to powders in the suspension. When the pH value is changed, the ionisation of  $\text{NH}_4\text{PAA}$  absorbed on the surface of the particles will be affected, as well as the structure of the double-electrical layer. Thus, electrostatic repulsion energy and the zeta potential will be changed. Meanwhile, the steric stabilization energy is also affected by the pH value. Fig. 5 shows that, at the beginning of pH decrease, the electrosteric stabilization energy had almost no change, resulting in little increase of the viscosity. When the pH reached the IEP and was then decreased further, the

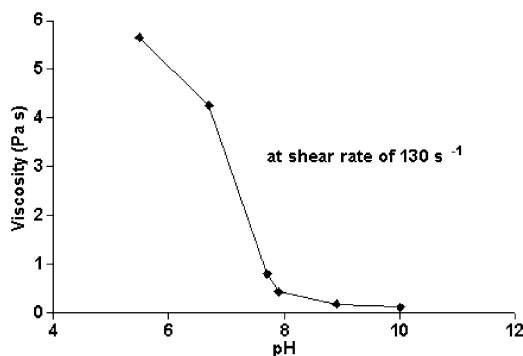


Fig. 5. Viscosity vs. pH of 75.0 wt.%, 0.14 wt.%  $\text{NH}_4\text{PAA}$  suspension.

electrosteric energy was affected strongly with a large increase observed in viscosity. Although the electrostatic repulsion energy should contribute to the stabilization while the suspension becomes more acid, the viscosity still increased. One possible explanation is that the steric effect introduced by the  $\text{NH}_4\text{PAA}$  may be damaged structurally around IEP and could not be recovered while the pH is reducing. Therefore, for the further study, there is no need to adjust the pH of the suspension since the viscosity of the intrinsic pH is suitable to the soft-molding microfabrication.

While changing the  $\text{NH}_4\text{PAA}$  concentrations of the 83.0 wt.% alumina suspensions, it was impossible to measure the viscosity for additions  $<0.10$  wt.%  $\text{NH}_4\text{PAA}$  as shown in Fig. 6. The suspensions with  $\text{NH}_4\text{PAA}$  of 0.14, 0.21 and 0.28 wt.% showed similar viscosity when shear rate was above  $100 \text{ s}^{-1}$ . It seemed that  $\text{NH}_4\text{PAA}$  of 0.14 wt.%, equalling to  $0.15 \text{ mg m}^{-2}$ , was the optimum concentration level for the 83.0 wt.% suspension. With increasing more  $\text{NH}_4\text{PAA}$ ,  $\text{NH}_4\text{PAA}$  would remain unabsorbed and then function as an electrolyte, which reduces the range and extent of the electrostatic repulsion force.

The relationship between the shear stress and shear rate, as well as between the viscosity and the shear rate of 83.0 wt.% alumina suspension with 0.14 wt.%

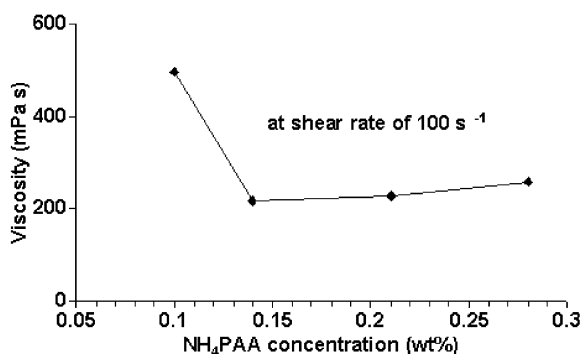


Fig. 6. Viscosity vs.  $\text{NH}_4\text{PAA}$  concentration of 83.0 wt.% alumina suspension at shear rate of  $100 \text{ s}^{-1}$ .

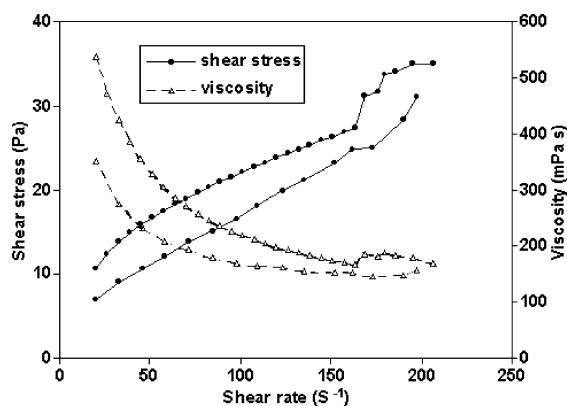


Fig. 7. Typical rheological flow behavior of 83.0 wt.% alumina suspension with 0.14 wt.%  $\text{NH}_4\text{PAA}$ .

$\text{NH}_4\text{PAA}$ , as shown in Fig. 7, present typical shear thinning or pseudoplastic curves. Commonly shear thinning conditions are convenient for processing as at low shear rates the viscosity is high enough to delay sedimentation, whilst at high shear rates the viscosity is low enough to produce a castable state.

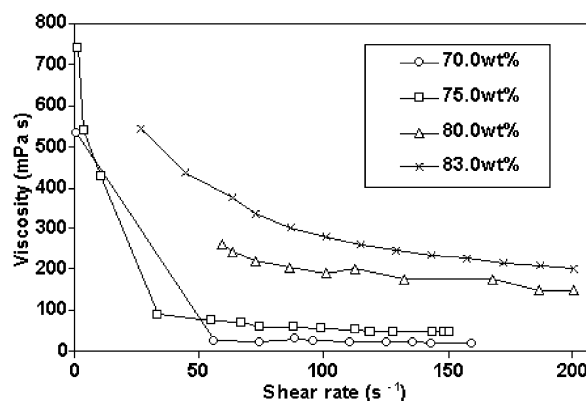


Fig. 8. Flow behaviour of alumina suspensions with 0.14 wt.%  $\text{NH}_4\text{PAA}$  of different solids loading.

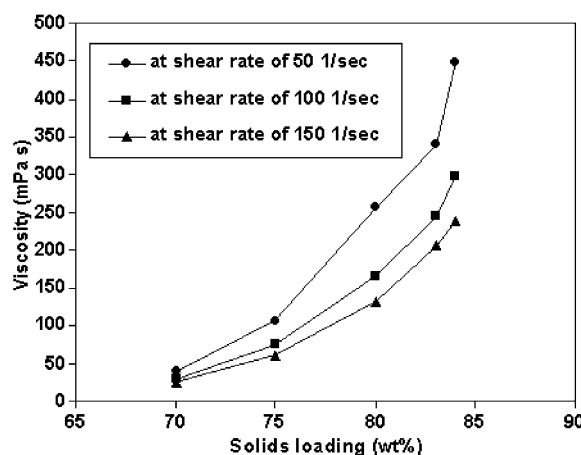


Fig. 9. Viscosities of alumina suspensions containing 0.14 wt.%  $\text{NH}_4\text{PAA}$  of different solids loading at different shear rates measured in shear stress mode.

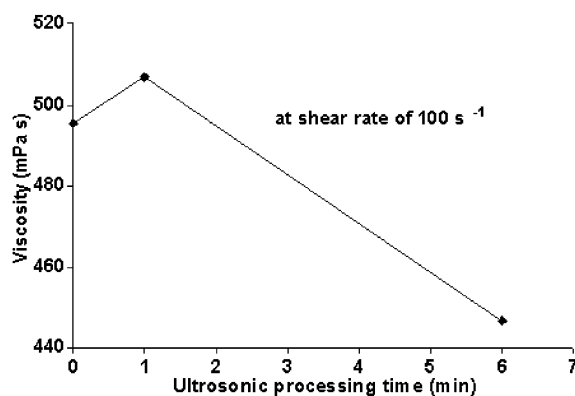


Fig. 10. Effect of ultrasonic processing on viscosity of 83.0 wt.%, 0.14 wt.%  $\text{NH}_4\text{PAA}$  suspension.



The viscosities of different solids loading suspensions are shown in Figs. 8 and 9. With solids loading of more than 80.0 wt.%, the viscosity raised dramatically and the measurement of the 84.0 wt.% suspension could not been performed in shear rate mode because of drying problems. It is very obvious in Fig. 9 that the viscosity of 84.0 wt.% suspension was almost 10-fold that of the 70.0 wt.% suspension. Noticeably the viscosity of the

highest solids loading suspension, 84.0 wt.% with 0.14 wt.%  $\text{NH}_4\text{PAA}$ , was just 0.30 and 0.45 Pa s at shear rates of 100 and 50  $\text{s}^{-1}$ , respectively. This means good fluidity and easy processing ability even for this high solids loading suspension.

The suspension of 83.0 wt.%, 0.14 wt.%  $\text{NH}_4\text{PAA}$  was processed with the ultrasonic processor by inserting the ultrasonic probe into the suspension, which was

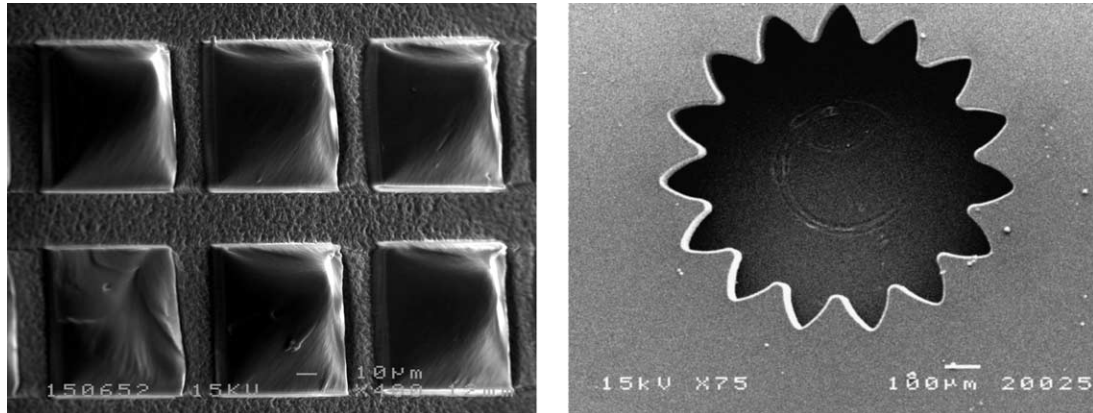


Fig. 11. Examples of the PDMS soft molds: (A) replicated from 200 mesh TEM copper grid; (B) replicated from SU-8 photoresist master.

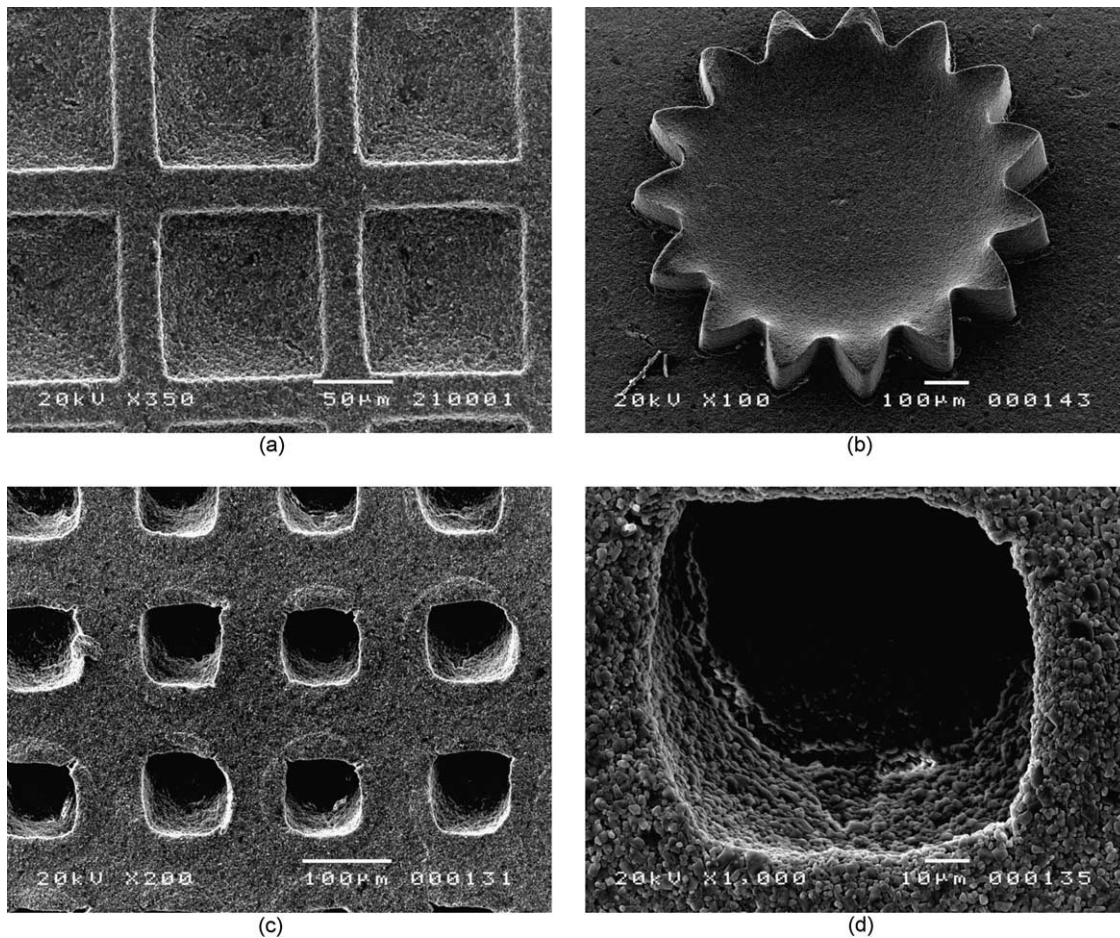


Fig. 12. SEM photos of the alumina microstructures after sintering: (a) TEM copper grid structure; (b) microgear; (c) microgrids array; (d) grain microstructures of the microgrid array.

surrounded by ice water to prevent a rise in temperature and water evaporation. With increasing the processing time, viscosity had almost no change, as shown in Fig. 10.

In terms of the embossing and microtransfer molding for the micropatterned structures, the 84.0 wt.% suspension with 0.14 wt.%  $\text{NH}_4\text{PAA}$  dispersant seems very suitable for processing with its viscosity of 0.30 Pa s at the shear rate of  $100 \text{ s}^{-1}$ , where the shear rate is similar to that used for molding work. By using the highest solid loading alumina suspension embossed using the PDMS molds show in Fig. 11, crack-free, very complete and dense microstructures with small shrinkage were obtained after sintering as shown in Fig. 12 (a) and (b). A microgrid structure is also shown in Fig. 12 (c) and (d). Resolution of these microstructures is around  $100 \mu\text{m}$  and the smallest in Fig. 12(a) is  $30 \mu\text{m}$ . The defects appearing on the upper part of grids in Fig. 12(c) are due to demolding the PDMS along this direction.

#### 4. Conclusion

The rheological properties of highly concentrated aqueous suspensions of A-16 SG  $\text{Al}_2\text{O}_3$  have been characterized with regard to pH, solids loading and dispersant concentration.  $\text{NH}_4\text{PAA}$  is very effective as a dispersant for this colloidal system by introducing electrosteric stabilization energy to prevent the agglomeration, with 0.14 wt.% being the best concentration for the very high solid loading systems. pH value also has strong influence on the stability of the high solid loading suspension and the flocculation happens while the pH shifts from the intrinsic point to the acidic region, indicating the IEP of 75.0 wt.%, 0.14 wt.%  $\text{NH}_4\text{PAA}$  suspension is around 7.0 and the intrinsic pH is suitable for this system and soft-molding.

A stable and easily processable suspension has been achieved with 0.30 Pa s viscosity at  $100 \text{ s}^{-1}$  shear rate for 84.0 wt.% solid loading with 0.14 wt.%  $\text{NH}_4\text{PAA}$  dispersant, and suitable for imprinting and microtransfer molding with the PDMS soft molds. Complete and dense microstructures have been demonstrated successfully on alumina substrates with resolution around  $100 \mu\text{m}$  and smallest of  $30 \mu\text{m}$ .

#### Acknowledgements

The authors would like to thank the British Council and the University of Birmingham for the ORS award (OZ) and research studentships. The authors are grateful to Dr. R. Greenwood in the Department of Chemical Engineering of the University of Birmingham for the help on the Zeta potential measurements. Also,

thanks to Mr. Geoff Dolman and Mr. Carl Meggs for technical assistance.

#### References

1. Kleinschmidt, P. and Hanrieder, W., The future of sensors, materials science or software engineering. *Sensor. Actuat A-Phys.*, 1992, **33**, 5–17.
2. Madou, M. J., *Fundamentals of microfabrication*. CRC Press, Boca Raton, FL, 1997.
3. Jawbson, S. C., Hergenroder, W., Koutny, L. B. and Ramsey, J. M., High-speed separation on a microchip. *Anal. Chem.*, 1994, **66**, 1114–1118.
4. Ehrfeld, W., Hessel, V. and Lehr, H., Microreactors for chemical synthesis and biotechnology—current developments and future applications. *Top. Curr. Chem.*, 1998, **194**, 233–252.
5. Wise, K. D. and Najafi, K., Microfabrication techniques for integrated sensors and microsystems. *Science*, 1991, **254**, 1335–1342.
6. Bryzek, J., Impact of MEMS technology on society. *Sensor. Actuat A-Phys.*, 1996, **56**, 1–9.
7. Liew, L.-A., Zhang, W., An, L., Shah, S., Luo, R. L., Liu, Y. P., Cross, T., Dum, M. L., Bright, V., Daily, J. W., Raj, R. and Anseth, K., Ceramic MEMS—new materials, innovative processing and future applications. *Am. Ceram. Soc. Bull.*, 2001, **80**, 25–30.
8. Ehrfeld, W., Hessel, V., Lowe, H., Schulz, C. and Weber, L., Materials of LIGA technology. *Microsyst. Technol.*, 1999, **5**, 105–112.
9. Donohoe, K. G., Turner, T. and Jackson, K. A., Etching processes in semiconductor manufacturing. In *Materials Science and Technology*, Vol. 16, (Chapter 6), ed. R. W. Cahn, P. Haasen, E. J. Kramer and K. A. Jackson. VCH Publishers Inc, New York, 1996.
10. Eidelloth, W., Gallagher, W. J., Robertazzi, R. P., Koch, R. H., Oh, B. and Sandstrom, R. L., Wet etch process for patterning insulators suitable for epitaxial high-T superconducting thin film multilevel electronic circuits. *Appl. Phys. Lett.*, 1991, **59**, 1257–1259.
11. Rousseau, F., Jain, A., Kodas, T. T., Hampden-Smith, M., Farr, J. D. and Muenchhausen, R., Low-temperature dry etching of metal oxides and ZnS via formation of volatile metalbeta-diketone complexes. *J. Mater. Chem.*, 1992, **2**, 893–894.
12. Wang, S., Li, X., Wakabayashi, K. and Esashi, M., Deep reactive ion etching of lead zirconate titanate using sulfur hexafluoride. *J. Am. Ceram. Soc.*, 1999, **82**, 1339–1341.
13. Van-Hoy, C., Barda, A., Griffith, M. and Halloran, J. W., Microfabrication of ceramics by co-extrusion. *J. Am. Ceram. Soc.*, 1998, **81**, 152–158.
14. Wang, S., Li, J.-F., Watanabe, R. and Esashi, M., Fabrication of lead zirconate titanate microrods for 1-3 piezocomposites using hot isostatic pressing with silicon molds. *J. Am. Ceram. Soc.*, 1999, **82**, 213–215.
15. Chen, R. H. and Lan, C. L., Fabrication of high-aspect-ratio ceramic microstructures by injection molding with the altered lost mold technique. *J. Microelectromech. S.*, 2001, **10**, 62–68.
16. Halloran, J. W., Freeform fabrication of ceramics. *Brit. Ceram. T.*, 1999, **98**, 299–303.
17. Knitter, R., Bauer, W. and Gohring, D., Manufacturing of ceramic microcomponents by a rapid prototyping process chain. *Adv. Eng. Mater.*, 2001, **3**, 49–54.
18. Sachs, E., Cima, Williams, P., Brancazio, D. and Cornie, J., Three dimensional printing: rapid tooling and prototypes directly from a CAD model. *J. Eng. Ind.-T. ASME*, 1992, **114**, 481–488.
19. Bladzell, P. F., Evans, J. R. G., Edirisinghe, M. J., Shaw, P. and Binstead, M. J., The computer aided manufacture of ceramics

- using multiplayer jet printing. *J. Mater. Sci. Lett.*, 1995, **14**, 1562–1565.
20. Tay, B. Y. and Edirisinghe, M. J., Investigation of some phenomena occurring during continuous ink-jet printing of ceramics. *J. Mater. Res.*, 2001, **16**, 373–384.
21. Mott, M. and Evans, J. R. G., Zirconia/alumina functionally graded material made by ceramic ink jet printing. *Mat. Sci. Eng. A-Struct.*, 1999, **271**, 344–352.
22. Griffith, M. L. and Halloran, J. W., Freeform fabrication of ceramics via stereolithography. *J. Am. Ceram. Soc.*, 1996, **79**, 2601–2608.
23. Hinczewski, C., Corbel, S. and Chartier, T., Ceramic suspensions suitable for stereolithography. *J. Eur. Ceram. Soc.*, 1998, **18**, 583–590.
24. Bourell, D. L., Marcus, H. L., Barlow, J. W. and Beaman, J. J., Selective laser sintering of metals and ceramics. *Int. J. Powder Metall.*, 1992, **28**, 369–381.
25. Subramanian, P. K. and Marcus, H. L., Selective laser sintering of alumina using aluminium binder. *Mater. Manuf. Process.*, 1995, **10**, 689–706.
26. Bauer, W., Ritzhaupt-Kleissl, H.-J. and Hausselt, J., Micro-patterning of ceramics by slip pressing. *Ceramics International*, 1999, **25**, 201–205.
27. Schonholzer, U. P., Hummel, R. and Gauckler, L. J., Micro-fabrication of ceramics by filling of photoresist molds. *Adv. Mater.*, 2000, **12**, 1261–1263.
28. Biebuyck, H. A., Larsen, N. B., Delamarche, E. and Michel, B., Lithography beyond light: microcontact printing with monolayer resists. *IBM J. Res. Dev.*, 1997, **41**, 159–170.
29. Xia, Y. and Whitesides, G. M., Soft lithography. *Angew. Chem., Int. Ed. Engl.*, 1998, **37**, 550–575.
30. Cesarano III, J. and Aksay, I. A., Processing of highly concentrated aqueous  $\alpha$ -alumina suspensions stabilized with polyelectrolytes. *J. Am. Ceram. Soc.*, 1988, **71**, 1062–1067.
31. Lewis, J. A., Colloidal processing of ceramics. *J. Am. Ceram. Soc.*, 2000, **83**, 2341–2359.
32. Davies, J. and Binner, J. G. P., The role of ammonium polyacrylate in dispersing concentrated alumina suspensions. *J. Eur. Ceram. Soc.*, 2000, **20**, 1539–1553.
33. Greenwood, R., Roncari, E. and Galassi, C., Preparation of concentrated aqueous alumina suspensions for tape casting. *J. Eur. Ceram. Soc.*, 1997, **17**, 1393–1401.